Resources, Conservation & Recycling 149 (2019) 372–380

Contents lists available at ScienceDirect

Resources, Conservation & Recycling

journal homepage: www.elsevier.com/locate/resconrec

Full length article

Utilization of coal fly and bottom ash pellet for phosphorus adsorption: Sustainable management and evaluation

Hongxu Zhou[a,b], Rabin Bhattarai[a,*], Yunkai Li[b], Shiyang Li[c], Youheng Fan[a]

[a] Department of Agricultural and Biological Engineering, University of Illinois at Urbana-Champaign, Urbana, IL61801, USA
[b] College of Water Resources and Civil Engineering, China Agricultural University, Beijing, 100083, PR China
[c] College of Environmental Science and Engineering, Tongji University, Shanghai, 200092, PR China

ARTICLE INFO

Keywords:
Coal ash reuse
Pelletized adsorbent
Foaming
Phosphate removal
Heavy metal leaching

ABSTRACT

Recycling of coal combustion solids can have several environmental benefits. The objective of this study was to evaluate a sustainable approach to recycle coal fly ash and bottom ash as pelletized-adsorbents for dissolved phosphorus (P). Sodium Dodecyl Sulfate (SDS), a foaming agent, was added to enhance the phosphorus adsorption capacity of fly ash pellets (FAP) and bottom ash pellets (BAP) during the pellet fabrication. Ten types of fly ash pellets and bottom ash pellets with varying Sodium Dodecyl Sulfate proportions (FAP-0/BAP-0: 0% SDS; FAP-1/BAP-1: 2% SDS; FAP-2/BAP-2: 4% SDS; FAP-3/BAP-3: 6% SDS; FAP-4/BAP-4: 8% SDS by weight) were manufactured with a high temperature (700°C) modification process. The results indicated that the bottom ash pellet was more suitable adsorbent than fly ash pellet due to the better phosphorus adsorption capacity and lower heavy metal leaching. After the addition of Sodium Dodecyl Sulfate, the volumetric porosity of fly ash pellets and bottom ash pellets increased by 45.5%–163.6%, 52.9%–76.5%, respectively. However, higher Sodium Dodecyl Sulfate fraction did not result in better pellet phosphorus removal, since FAP-2 and BAP-3 resulted in the highest phosphorus removal among the pellets tested in this study. The results from X-ray diffraction demonstrated that Calcium and Silica were the major phases in the pellets. This study provides a feasible approach to reuse fly ash and bottom ash as effective pelletized-adsorbents for water quality improvement. These pellets can be applied in edge-of-field and in-stream treatment to control P loss from the agricultural area.

1. Introduction

Coal combustion process generates an enormous amount of solid waste such as fly ash and bottom ash (Agriz et al., 2018). The inappropriate and unsustainable methods to dispose of these ashes not only consume a lot of human and financial resources, but also lead to serious environmental pollution problem (Lemly, 2015). Many approaches have been recommended in the literature to dispose those ashes as recyclable resources, such as applying them in construction material (Xu and Shi, 2018; Singh and Arya, 2019) or using as eco-friendly fillers in synthetic rubber for tire (Ren and Sancaktar, 2019). Reusing them to eliminate different pollutants from water would solve the serious environmental and sustainability issues, such as water quality and waste management problems.

Attention has been focused on utilizing fly ash for contamination removal many years, especially for phosphorus (P) removal (Ahmaruzzaman, 2010; Hermassi et al., 2017; Li et al., 2018). The excessive input of P into water could cause water pollution (i.e. eutrophication), posing threats to the ecosystems and resulting in economic loss (Conley et al., 2009). As an inexpensive byproduct, fly ash contains a large number of metal oxides such as Calcium (Ca), Aluminum (Al) and Iron (Fe) oxides making it an ideal adsorbent for P removal from agricultural and industrial wastewater (Allred, 2010). For example, Lu et al. (2009) studied the effectiveness of fly ash in removing phosphate from aqueous solution and related removal mechanism, and their results showed that the removal percentage of phosphate in the first 5 min reached 68–96%. Ragheb (2013) concluded that fly ash reached maximum phosphate adsorption at a neutral pH value of seven. As for bottom ash, earlier studies have demonstrated that bottom ash has a similar adsorption capacity as fly ash (Sun et al., 2008; Chong et al., 2009). Chimenos et al. (1999) evaluated the potential applications of bottom ash and its environmental hazards, whereas Lin and Yang (2002) investigated the adsorption characteristic of bottom ash for reducing the concentrations of various contaminants and concluded that it was possible to use bottom ash for removing pollutants. However, the utility value of bottom ash as P adsorbent

* Corresponding author.
E-mail address: rbhatta2@illinois.edu (R. Bhattarai).

https://doi.org/10.1016/j.resconrec.2019.06.017
Received 19 March 2019; Received in revised form 6 June 2019; Accepted 12 June 2019

remains unknown due to a limited investigation to compare the P removal efficiency of fly ash and bottom ash.

Although fly and bottom ash have a potential for P removal, they may contain some trace heavy metals such as Lead (Pb), Chromium (Cr), Arsenic (As), Cadmium (Cd) and Mercury (Hg). These heavy metals could be toxic to human and ecosystems even at relatively low concentrations (Colangelo et al., 2012). In addition, the powder-form of ashes can cause dust pollution during transportation and are difficult to collect from contaminant water after P removal. These two reasons restrict the practical application of fly and bottom ash for P removal.

Some researchers used the pelleting technique to create an adsorbent for P removal from wastewater (Littler et al., 2013; Li et al., 2018). Li et al. (2017) used fly ash as the primary material to create ceramic pellets to remove dissolved P. Furthermore, this pellet-form sorbent can be incorporated into an edge-of-field practice (Li et al., 2018). Hence, the pelletization provides a feasible way of using fly and bottom ashes in P removal with better handling, lower transportation, storage costs, and easier recycling.

Porosity is one of the crucial factors that influence the physical interactions and chemical reactivity of solids with liquids. Khelifi et al. (2002) mixed zeolitized fly ash and slag to obtain carriers with larger porosity to remove P on the aquatic environment. As a matter of fact, in environmental and biomedical industries, the direct foaming method offers a simple and inexpensive way to increase porosity (Han et al., 2011; Lakshmi et al., 2015). However, the use of a foaming agent to improve the P adsorption efficiency of fly ash and bottom ash pellets has not been investigated yet to our knowledge. Thus, there is a need to examine the potential of a foaming agent to gain a better P removal efficiency for the pellet.

The objective of this study was to investigate a sustainable approach to recycle coal fly ash and bottom ash in an eco-friendly way. Fly ash pellet (FAP) and bottom ash pellet (BAP) were manufactured and their viability and effectiveness for P adsorption were evaluated. An inexpensive and effective foaming agent (sodium dodecyl sulfate, SDS) was employed to improve the porosity of the FAPs and BAPs. In addition, heavy metal (Pb, Cr, As, Cd, Hg) leaching from raw fly/bottom ashes and fly/bottom ash pellets was also investigated to assess the potential of fly and bottom ash pellets as eco-friendly adsorbents.

2. Materials and methods

2.1. Raw materials

Fly and bottom ash were obtained from a power plant at Chenzhou city, Hunan Province, China. The appearance and surface structure of fly and bottom ash indicated that fly ash had a much finer texture than bottom ash (Fig. 1). The density of fly and bottom ash was measured to be 1318.2 kg/m^3 and 1423.1 kg/m^3, respectively. The chemical composition of fly and bottom ash were analyzed using X-ray fluorescence spectrometer (Table.S1). Clay and lime are two commonly used materials as a binding agent for shaping pellets. Fine bentonite clay was obtained from Nature's Oil Company (Ohio, USA). The density of clay powder was measured to be 801.1 kg/m^3. The lime powder was acquired from Waukesha Lime and Stone, Wisconsin, USA. The density of lime powder was measured to be 1190.24 kg/m^3. A surfactant, sodium dodecyl sulfate (SDS, > 99%, flash point 170 °C, Sigma-Aldrich Co., USA), was used as the foaming agent in this study.

2.2. Pellet fabrication

Based on the findings of a previous study (Li et al., 2017), the original pellet mixture contained 60% of fly/bottom ash, 30% of lime powder and 10% of clay powder, by weight, respectively. Five different proportions (0% 2%, 4%, 6%, 8%, by weight) of SDS were measured and added to the deionized water. The pellet with 60% fly/bottom ash, 30% lime and 10% clay without SDS was used as the control and labeled as FAP-0 or BAP-0. Subsequently, the pellet mixture with varying amount of SDS (FAP-1: SDS 2%, FAP-2: SDS 4%, FAP-3: SDS 6% FAP-4: SDS 8%; BAP-1: SDS 2%, BAP-2: SDS 4%, BAP-3: SDS 6% BAP-4: SDS 8%) were prepared.

The dry materials (fly/ bottom ashes, lime, and clay) were mixed uniformly in the beginning. SDS solution was added into the mixture to prepare the slurry and stirred for 5 min in a household mixer, after which the slurry mix was wrapped in Clingfilm and allowed to foam and stabilize for 24 h at room temperature. Then, the slurry was shaped into pellets using a pellet press (Parr instrument Co, USA). The pellets were cylindrical in shape with approximately 0.5 cm diameter and 1 cm long (Fig. 2). An earlier study indicated that more Ca, Fe and Al were released from the crystal matrix at 700°C than other temperature, which would promote phosphorus sorption (Gan et al., 2009). Hence, we selected 700°C as the temperature for the thermal modification process in this study. The pellets were baked in a high-temperature furnace (Thermolyne BOX furnace, MA, USA) for 10 h in total, raising the temperature 100 °C each hour for 6 h, and then keeping it at 700 °C for another 4 h. The pellets were cooled down for 6 h after taking out from the furnace and washed with distilled water.

2.3. Pellet characterization

The volumetric porosity (Φv) and surface porosity (Φ_A) were calculated by the following equations (Eq. (1) and (2)). (Zhang et al., 2017)

$$\Phi_v = 1 - \frac{\rho_{pellet}}{\rho_{material}} \quad (1)$$

$$\Phi_A = (1 - \frac{\rho_{pellet}}{\rho_{material}})^{2/3} \quad (2)$$

Where ρ_{pellet} = density of the pellet; $\rho_{material}$ = density of fly ash, clay, and lime mixture. The units of Φv and Φ_A are %.

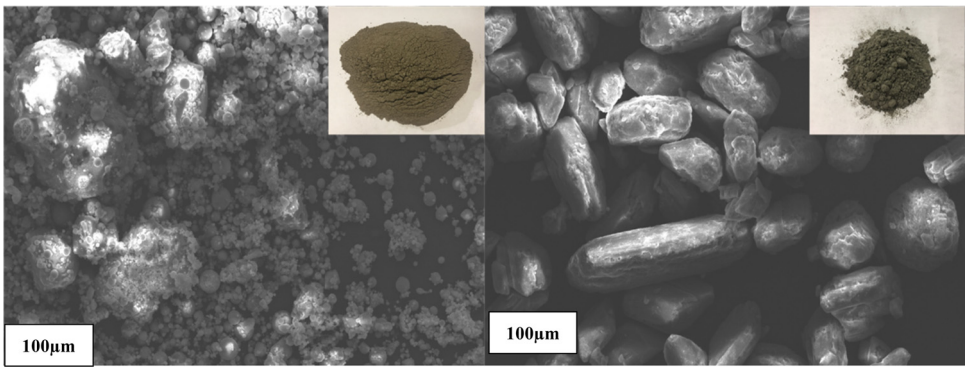

Fig. 1. Appearance and surface structure of fly ash (left) and bottom ash (right).

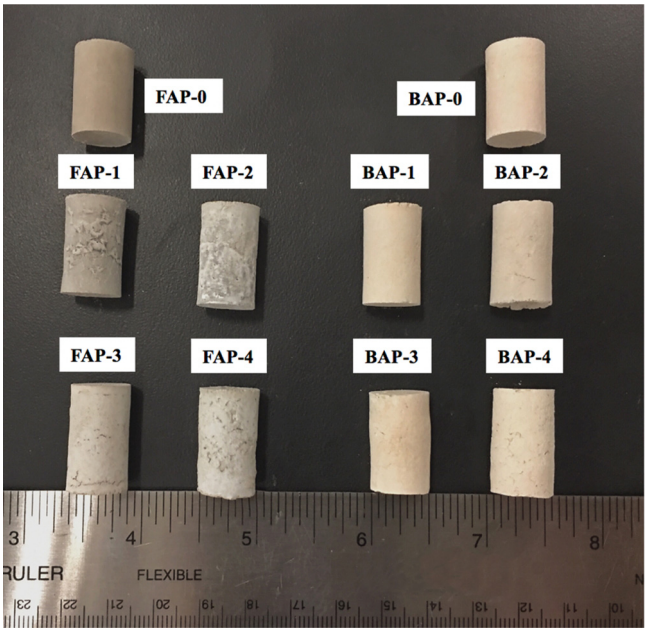

Fig. 2. Fly ash and bottom pellets with different ratio of SDS.

The X-ray diffraction (XRD) technique was used to distinguish the crystalline and non-crystalline nature of the pellets. XRD of the fly ash and bottom ash pellets was performed using a Panalytical X'Pert MRD system, with Cu K-alpha (0.15418 nm) x-rays in point focus, a Ni filter to block Cu K-beta x-rays, and 0.27 ° parallel plate secondary collimators. X-ray power settings were 45 kV and 40 mA. The scan step size was 0.05 degrees, with 4-second integration time per point. The XRD diffractions identified $CaCO_3$, $CaSO_4$, and SiO_2 as major constituents for the pellets which demonstrated that the fly ash pellets and bottom ash pellets would release a relatively high total Ca^{2+} concentration in the solution. An FEI Quanta FEG 450 Environmental Scanning Electron Microscopy (ESEM) was also used to analyze the surface structure and microphotography of the pellets.

2.4. P adsorption experiment

A series of P adsorption experiments were conducted following the ASTM standard procedure (D4646-87). Each type of pellets was tested with three replications. Since the orthophosphate is the primary form of phosphorus responsible for eutrophication (Wei et al., 2008), Potassium phosphate monobasic (KH_2PO_4, CAS#: 7778-77-0, acquired from Sigma-Aldrich, USA) was used in adsorption tests as the source of orthophosphate.

In each adsorption experiment, 10 g of the pellet was measured with a digital scale and shaken at 120 rpm in the 100 ml of 1.0 mg/l phosphate solution at the room temperature. After placing the pellets in the solution, 5 ml of water samples were collected after 30 s, 1 min, 2 min, 5 min, 10 min, 30 min, 60 min, and 90 min. Then, the phosphate concentrations in the solution samples were determined using a continuous flow Technicon Autoanalyzer II system following EPA method 365.1 (USEPA, 1993) procedures. After completion of the absorption test, all pellets were filtrated and put into flasks with 100 ml DI water for desorption and heavy metal leaching tests. Flasks were placed at the shaker for 24 h with a 120-rpm speed at room temperature (Li et al., 2017). The solution samples were collected after 24 h. The heavy metals (Pb, Cr, As, Cd, Hg) released from the samples was analyzed using Inductively Coupled Plasma mass spectrometry (ICP- MS) and phosphate concentrations of samples after desorption were measured at the same time. Meanwhile, the same experimental step was used to quantify the heavy metal leaching from the raw fly ash and bottom ash. Due to the expensive sample analysis cost, we mixed the multiple samples and the representative value was reported.

The effect of pH on the uptake of P from aqueous solution by the fly and bottom ash pellets was investigated. Following the testing procedure of published literature (Li et al., 2017; Cui et al., 2018), the solution pH was varied from 4 to 10 by using an appropriate amount of hydrochloric acid (HCl) and potassium hydroxide (KOH). 4 g of the pellet was added to the 100 ml phosphate solution (40 mg/l) with pH 4 to 10, respectively. The flasks were shaken at 120 rpm for 24 h to attain equilibrium, and the samples were collected to measure the phosphate concentration. The pH of the solutions was measured using a Fisher Scientific™ Accumet™ AE150 pH Benchtop Meter.

2.5. Adsorption isotherms

Adsorption isotherms express the relationship between the mass of P adsorbed at constant temperature per unit mass of the fly/bottom ash pellets and the liquid phase P concentration. To quantify the P sorption capacity of pellet, the Langmuir, Freundlich, and Tempkin isotherms were applied in this study. 4 g of the pellet was placed in a 100 ml P solution with seven concentrations (0.5,1,2,5,10,50 and 100 mg/l) and put in the shaker for 24 h with 120 rpm. Then the pellets were filtered out from the solution, and the P concentration in the solution was measured to fit the adsorption isotherms.

Langmuir isotherm model determines the adsorption of ions on the surface of the adsorbent on the monolayer and equivalent sites on the surface (Kundu and Gupta, 2006; Mor et al., 2016) Langmuir isotherm can be expressed as follows:

$$\frac{C_e}{q_e} = \frac{1}{q_{max}} b + \frac{C_e}{q_{max}} \tag{3}$$

$$R_L = \frac{1}{1 + bC_o} \tag{4}$$

Where q_e is the total amount of P adsorbed on the pellet at equilibrium (mg/g); *Ce* is the solution concentration at equilibrium (mg/L); *b* is Langmuir constant (L/mg), *qmax* represents total number of binding sites or alternatively represents the maximum amount of ion per unit mass of adsorbent; R_L means the separation constant, which can be used to predict whether the sorption is “favorable” or “unfavorable”; C_O is the initial concentration (mg/L).

The Freundlich isotherm model is an empirical equation assuming that the adsorption process takes place on a heterogeneous surface (Badruzzaman et al., 2004). It is can be defined as below:

$$\log Q_e = \log k + \frac{1}{n} \log C_e \tag{5}$$

Where *k* is Freundlich constant that depends upon the nature of adsorbate(P) and adsorbent (fly/bottom ash pellets) and *n* indicates the adsorption capacity of adsorbent and the intensity of adsorption.

Tempkin isotherm model involves a factor that allows for interactions between adsorbents and adsorbates (Rangabhashiyam et al., 2014). The Tempkin model is represented by the following equation:

$$q_e = B_1 \ln K_T + B_1 \ln C_e \tag{6}$$

Where K_T is equilibrium binding constant and B_1 related to the heat of the adsorption. The valued of K_T and B_1 are obtained by using linear plot q_e against the ln *Ce*.

2.6. Statistical analysis

Statistical analysis was performed using a one-way analysis of variance (ANOVA). P-values less than 0.05 was considered statistically significant. SPSS statistics 17.0 software was used to conduct the statistical analysis.

Table 1
Physical properties of pellets (unit %).

Ash type	Ash: Clay: Lime	SDS	Volumetric porosity (Φv)	Surface porosity (Φ_A)
FAP-0	60:10:30	0	11 ± 3	23 ± 4
FAP-1	60:10:30	2	24 ± 2	39 ± 2
FAP-2	60:10:30	4	29 ± 2	44 ± 2
FAP-3	60:10:30	6	28 ± 2	42 ± 2
FAP-4	60:10:30	8	16 ± 2	29 ± 3
BAP-0	60:10:30	0	17 ± 2	31 ± 6
BAP-1	60:10:30	2	26 ± 2	41 ± 2
BAP-2	60:10:30	4	27 ± 2	42 ± 2
BAP-3	60:10:30	6	30 ± 2	45 ± 2
BAP-4	60:10:30	8	28 ± 2	43 ± 2

3. Results and analysis

3.1. Effect of SDS on fly ash and bottom ash pellets

Porosity calculations indicated that the volumetric porosity (Φv) and surface porosity (Φ_A) of different types of FAPs and BAPs varied significantly (Table 1). After adding SDS, the Φv of FAPs and BAPs increased by 45.5%–163.6%, 52.9%–76.5%, respectively. Moreover, the Φ_A of FAPs and BAPs increased by 26.1%–91.3% and 32.2%–45.1%, respectively, compared to FAP-0 and BAP-0. The results also indicated that the more SDS added to the mixture did not result in the higher porosity. For FAPs, Φv and Φ_A for FAP-0 were calculated to be 11% and 23%, respectively. After increasing the ratio of SDS, Φv and Φ_A increased up to approximately maximum of 29% and 44%, respectively, at 4% of SDS, then they decreased and reached around 16% and 29%, at 8% of SDS. Similar trends were also found for BAPs. The highest Φv and Φ_A were obtained for BAP-3 at the addition of 6% SDS, around 30% and 45%, respectively. Subsequently, Φv and Φ_A decreased to 28% and 43% when the SDS proportion was increased to 8%.

The ESEM was applied to analyze the effect of SDS on pellet surface structure (Fig. 3a-d). The pellets without using SDS (FAP/BAP-0) and the pellets with the highest porosities (FAP-2, BAP-3) were selected for the analysis. Fig.3a-b presented the microstructure of two types of pellets without the addition of SDS. The relatively smooth and uniform surface structure was observed for FAP-0 and BAP-0. These pellets exhibited microstructure homogeneity and constituted compact materials. In contrast to the FAP/BAP-0, the surface structure for FAP-2 (with 4% SDS) and BAP-3 (with 6% SDS) pellets possessed rough and wrinkled surface morphology, had porous and cavities and interspaces, potentially providing more adsorption sites for P (Fig. 3c-d). These two pellets with higher porosity (Φv, Φ_A) exhibited higher permeability, excellent adsorptive capacity and rough surface, which were more suitable as P adsorbents than those with small porosity. Meanwhile, by analyzing the surface structure of FAP-0 and BAP-0 in Fig.3a-b, the BAP-0 had a rougher surface compared to FAP-0, which indicated that BAP might obtain a better P adsorption capacity than FAP.

3.2. Pellets kinetic test

The laboratory results illustrated that P concentration in the solution fell rapidly after the addition of FAPs and BAPs, but the rates of change in P concentration were different for each pellet (Fig. 4). Among five types of FAPs, the FAP-2 had the highest adsorption efficiency with P concentration reduction by 65% and the FAP-0 showed the lowest adsorption efficiency with only 25% reduction in P concentration within 10 min (Fig. 4a). Similarly, BAP-3 had the highest adsorption efficiency with the P concentration reduction by 76%, and the BAP-0 showed the minimum adsorption efficiency (46%) among five BAPs tested within 10 min (Fig. 4b). At the end of the batch test, almost all dissolved P (> 92%) in the solution was adsorbed. P uptake capacity of the five types of FAPs tested was in the following order: FAP-2 > FAP-3 > FAP-1 > FAP-4 > FAP-0. Similarly, the P removal ability of the five kinds of BAPs tested was in the following order: BAP-3 > BAP-2 > BAP-4 > BAP-1 > BAP-0. By comparing the P removal efficiency of FAP and BAP under the same SDS ratio, the adsorption

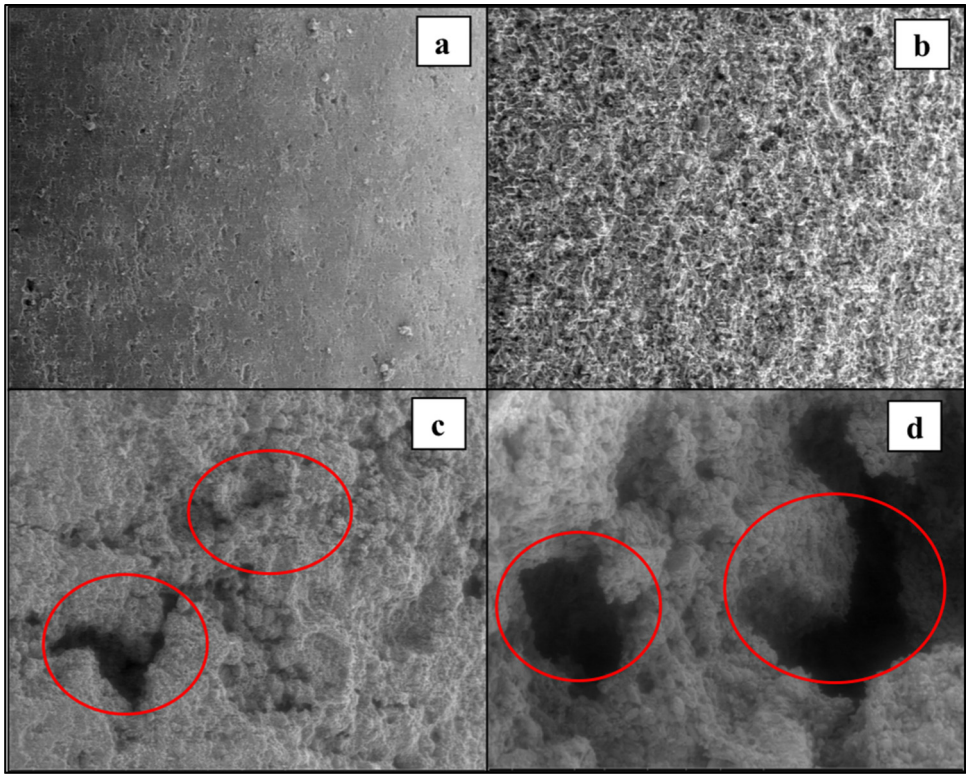

Fig. 3. The microphotographs of FAPs and BAPs using Environmental Scanning Electron Microscopy: (a) FAP-0, (b) BAP-0, (c) FAP-2, (d) BAP-3 (500 μm).

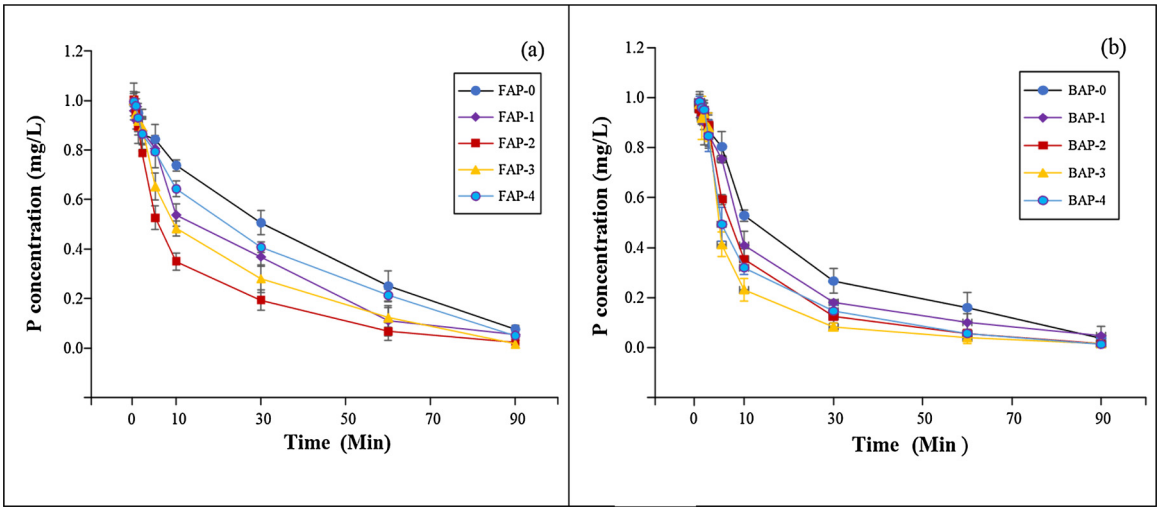

Fig. 4. P removal during kinetic test test for: (a) 5 types of FAPs. (b) 5 types of BAPs.

performance of BAP was found to be better than that of FAP.

Similar P removal tendencies were observed in previous studies (Littler et al., 2013; Li et al., 2017). This result indicated that using SDS could significantly improve P adsorption performance. However, it did not mean the more SDS added into the pellets resulted in the better adsorption ability. FAP-4 and BAP-4 both had the highest proportion of SDS among the pellets, but their P adsorption capacities were lower than FAP-2, FAP-3, FAP-1 and BAP-3, BAP-2, respectively. An explanation for this phenomenon has been provided in the discussion section.

3.3. Adsorption equilibrium

Analysis of equilibrium data is essential for understanding the adsorption of P over FAPs and BAPs. The experimental data was applied to Langmuir, Freundlich, and Tempkin isotherm models to find out the best-fit model. The observed data and correlation coefficient (R^2) for the isotherm models are presented in Table 2. For five types of FAPs, the highest correlation coefficient (R^2) was obtained for Freundlich equation, which indicated that the Freundlich model was the most suitable to describe the P sorption process with fly ash pellets, as reported by earlier studies (Lu et al., 2009; Ragheb, 2013). The Freundlich constant K ranged from 0.47 to 0.61, illustrating the variations in the phosphate adsorption capacity of different fly ash pellets. The *Qmax* value was the highest for FAP-2 among five FAPs tested, which was validated by the adsorption results. The adsorption of P on BAPs followed the Langmuir isotherm better, indicating that the sorption process of P on BAPs was more likely to be monolayer sorption on the surface. The *Qmax* values predicted by Langmuir isotherms can be used to evaluate the P adsorption capacities of BAPs. The sorption on BAPs was favorable under the batch experiment since the calculated R_L values (ranging from 0.003 to 0.005) were lower than 1. The R^2 values obtained for Temkin model indicated that the Temkin model does not fit the data well and it may not be the appropriate model to describe the P adsorption process in the pellets.

3.4. Effect of initial pH

The pH is a critical factor that affects the P absorption process on the pellets. The effect of initial pH on the adsorption of P from aqueous solution is illustrated in Fig. 5. The P uptake for both FAPs and BAPs increased with the increase in pH. The average rate of increase in P sorption for various FAPs and BAPs were 58% and 69%, respectively when the pH increased from 4 to 10. The maximum sorption capacity (2.56 mg/g) was observed for BAP-3 at pH 10 indicating that the P adsorption was more efficient under an alkaline condition and it declined with the decrease in pH of the aqueous solution. This observation is similar to other reports showing that P adsorption is more efficiently in alkaline solution when related to CaO-rich adsorbents (Pengthamkeerati et al., 2008; Li et al., 2017). Since the alkaline environment is a favorable condition for calcium phosphate precipitation (Gustafsson et al., 2012), it might lead to the formation of a number of Ca–P minerals, such as amorphous calcium phosphate, octa calcium phosphate, and apatite.

3.5. Heavy metal leaching and P desorption tests

The concentration of heavy metals released from raw ashes and fly/

Table 2
Isotherm parameters for phosphate sorption on the fly and bottom ash pellets from isotherm models.

Models	Parameters	Adsorbents									
		FAP-0	FAP-1	FAP-2	FAP-3	FAP-4	BAP-0	BAP-1	BAP-2	BAP-3	BAP-4
Langmuir	Q_{max} (mg/g)	0.59	1.47	2.56	1.86	1.49	0.98	1.23	2.32	2.56	1.64
	b (L/mg)	5.18	5.38	10.47	13.34	10.67	3.09	2.82	2.51	2.07	2.84
	R^2	0.95	0.89	0.53	0.76	0.87	0.99	0.98	0.98	0.99	0.98
	R_L	0.04	0.02	0.01	0.01	0.01	0.003	0.004	0.004	0.005	0.004
Freundlich	K(mg/g)	0.47	0.61	0.58	0.57	0.50	0.55	0.57	0.76	0.95	0.58
	n	2.05	2.04	1.29	1.39	1.49	1.63	1.49	1.57	2.02	1.17
	R^2	0.99	0.97	0.98	0.99	0.99	0.85	0.86	0.97	0.95	0.72
Tempkin	B (J/mol)	0.08	0.14	0.32	0.25	0.19	0.15	0.18	0.27	0.29	0.26
	K_T	5.75	2.67	4.92	2.95	3.93	7.92	7.84	26.84	239.85	5.87
	R^2	0.91	0.72	0.76	0.85	0.83	0.95	0.97	0.82	0.81	0.88

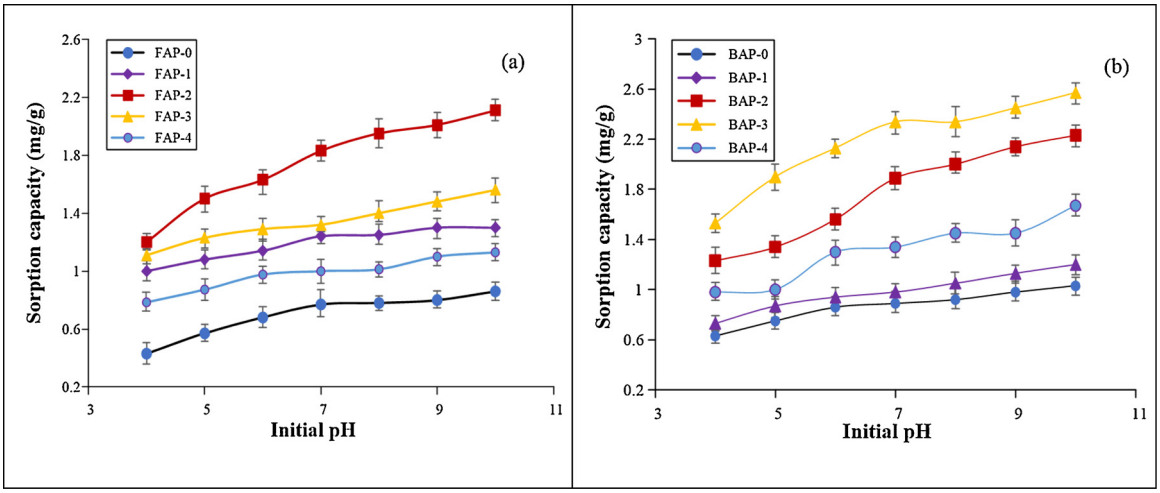

Fig. 5. Effect of initial pH on sorption capacity of pellet: (a) 5 types of FAPs. (b) 5 types of BAPs.

Table 3
Concentration of heavy metals and P released from raw fly/bottom ashes and fly/bottom ash pellets.

Elements	Limit concentration (μg/l)	Fly ash	bottom ash	Adsorbents									
				FAP-0	FAP-1	FAP-2	FAP-3	FAP-4	BAP-0	BAP-1	BAP-2	BAP-3	BAP-4
As	10.0	137.0	45.0	8.1	0.7	2.8	2.5	2.6	1.5	2.9	1.9	3.7	3.5
Cd	5.0	17.0	1.0	0.8	0.1	0.3	0.2	0.6	0	0.1	0.1	0.2	0.1
Cr	100.0	3091.0	615.0	213.3	289.5	243.4	118.4	133.0	19.4	17.1	9.2	20.8	14.3
Hg	2.0	3.0	130.0	ND	ND	ND	ND	ND	ND	ND	ND	ND	ND
Pb	15.0	344.0	70.0	16.2	1.4	5.6	6.1	14.0	1.9	7.8	7.2	8.5	6.6
P	—	—	—	23.0	26.0	27.0	47.0	40.0	28.0	36.0	35.0	33.0	41.0

bottom ash pellets is provided in Table 3. The results showed that the highest leached concentrations of As, Cd, Cr, and Pb were measured from raw fly ash. According to the standard of heavy metals concentration in drinking water from the US Environmental Protection Agency (EPA) (National Primary Drinking Water Regulations (NPDWR, 2009), except for the Cd measured in raw bottom ash, other four heavy metal concentration measured in both raw fly and bottom ashes were higher than the recommended concentration. This observation indicated that the direct use of fly ash and bottom ash for P removal would result in heavy metal contamination. However, the amount of five heavy metals leached from the pellets were much smaller than those from the raw ashes. After palletization, the concentration of Hg could not be detected in all ten types of fly or bottom ash pellets. Only Cr concentration leached from five types of FAPs (FAP-0 to FAP-4) and Pb concentration released from FAP-0 pellet were higher than the recommended Cr and Pb concentrations. FAP-1 showed the highest Cr concentration among all kinds of pellets with about 2.9 times higher than the recommended Cr limit (100 μg/l). The heavy metal concentrations leached from five kinds of BAPs pellets were all under the recommended concentration.

The P concentration measured after desorption is listed in Table 3. The range of P concentration released from fly and bottom ash pellets were 23 to 47 μg/L. Since the natural levels of phosphate range from 5 to 50 μg/l (USEPA, 1995), the P leached from pellets should not cause environmental problem on water bodies.

4. Discussion

Recycling of coal combustion waste (coal ash) can have significant environmental and economic benefits. Utilization of abundant, low-cost coal fly ash and bottom ash as pelletized-adsorbents for water quality treatment can alleviate both air and water pollution problems.

4.1. High P adsorption capacities of the pellets compared to other materials

In this study, high P adsorption capacities observed for different pellets demonstrate the potential of using fly ash and bottom ash pellets for P removal in the agricultural and industrial wastewater. When compared with FAP/BAP-0, the P adsorption capacity and porosity of FAPs and BAPs improved after employing SDS. Nevertheless, our results also indicated the highest SDS fraction did not result in the highest P adsorption capacities for pellets since the porosity in pellets originates from different processing and synthesis routes. SDS, an inexpensive and effective surfactant, can reduce the surface tension (or interfacial tension) between liquid and solid (Lakshmi et al., 2015). With the increase in surfactant molecules in the aqueous solution, the pressure of the liquid membrane decreased after the bubble formation, and the bubble remained longer. However, if the concentration of SDS was continuously increased, the bubbles became larger and thinner, the resistance to external forces decreased, which reduced the stability of the bubble. At lower the surface tension, it was more difficult for the mixed substances (fly/bottom ash, lime, and clay) to bond together. This phenomenon is unconducive in making pellets and leads to repeated extrusion and shaping during the pelleting process, which also results in a decrease in porosity. Thus, the optimal appending proportion of SDS for making FAPs and BAPs ranged between 4%–6%. Overall, this difference suggests that the use of SDS changes the surfaces characteristics of pellet, which increases the porosity of pellets and consequently improves the P adsorption performance of pellets. Higher porosity leads to a better adsorption capacity as reported by previous studies (Khelifi et al., 2002; Asl et al., 2019). The maximum sorption capacities of FAP-2 and BAP-3 were measured to be 2.05 mg P g^{-1} and 2.56 mg P g^{-1}, respectively at pH 10. These values were compared with the sorption capacities of some other adsorbent materials for phosphate adsorption, such as nanoparticles, slags and carbon waste (Table S2). Although these values were obtained under different experimental conditions,

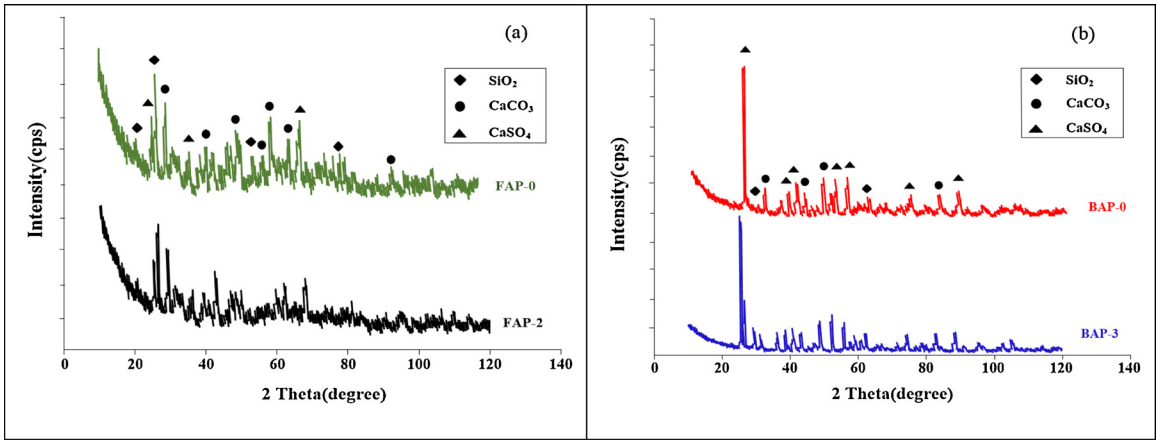

Fig. 6. XRD pattern of FAP-0, FAP-2, BAP-0 and BAP-3.

they can be used as a reference. The comparison demonstrates that the FAP and BAP can be applied as promising adsorbents for phosphate removal, because the adsorption capacities of FAP-2 and BAP-3 are higher than many of adsorbents such as rice husk (Mor et al., 2016), oyster shell (Chen et al., 2013) and coal cinder (Yang et al., 2009), and also the pellet-form provide a high potential and advantage to reuse waste solid.

4.2. P adsorption mechanism of the pellets

The XRD patterns of the four analysis samples are presented in Fig. 6. Diffraction patterns confirmed the presence of calcium (Ca) and observed to be the major phase among these four pellets. Several diffraction peaks of silica (Si) can be found at 20–30 2-Theta degree, consistent with the elemental composition results. The XRD diffractions identified $CaCO_3$, $CaSO_4$, and SiO_2 as major constituents based on the location of the peak. No apparent variations in crystalline peaks were detected after adding SDS, which indicated that the application of SDS did not change the main components and chemical properties of pellets.

Early studies have shown that the adsorbents rich in metal elements and silicon would remove P efficiently (Huang et al., 2017; Dai et al., 2017). Lu et al. (2009) revealed that calcium phosphate precipitation is a major mechanism of phosphate removal. In this study, the raw materials (ash, lime, and bentonite) provided large amounts of calcium and silicon for pellet fabrication. The presence of calcium ions and calcium carbonate could form stable Ca-P bond on the surface of pellets. Our result (Fig. 5) demonstrated that increase of pH exerted a positive influence on phosphate adsorption performance, which illustrated the presence of P chemisorption because an alkaline environment is a favorable condition for calcium phosphate precipitation (Gustafsson et al., 2012). The silicon provided by SiO_2 contributed to chemisorption and was more prone to form microporous structures in pellets to increase physical adsorption sites and consequently enhanced P physisorption capacity. On this basis, using SDS to increase the porosity of pellets can synergistically improve the physisorption and chemisorption capacities.

4.3. Analysis of heavy metal leaching from the pellets

The amount of heavy metal released from pellets is a crucial index to evaluate the pellets as eco-friendly adsorbents. According to our analysis (Table.3), the pelleting process with high-temperature thermal modification can significantly reduce the leaching of heavy metals from fly and bottom ash. There are three plausible reasons to explain the reduction of heavy metals leached from pellets. First, the formation of new phases and disappearance of earlier phases are two common phenomena during the pellets baking or sintering process (Guo et al., 2017). Heavy metals could be incorporated into the pellets via the melting process, and this consequently could inhibit the release of heavy metals from pellets. Many crystal phases containing heavy metals have been proved to possess good immobilization capacities, such as $PbAl_2Si_2O_8$ (Lu and Shih, 2012) and $CdAl_4O_7$ (Su et al., 2015). Second, previous studies indicated that carbonation is one of the most promising techniques to reduce the leaching of metals from coal ash (Sabbas et al., 2003; Van Gervem et al., 2005). Due to one of the mix materials is lime (mainly CaO), the combination of alkaline condition (Xuan and Poon, 2017) with the optimum carbonation temperature (700°C) (Song and Kim, 1990; Chen et al., 2007) can effectively decrease the leaching of heavy metals. Third, it was reported that the alkaline concentration would enhance the adsorption efficiency of coal ash for heavy metals (Wang et al., 2006), and a series of alkaline-modified fly ash and bottom ash can be used to remove heavy metal from wastewater (Koukouzas et al., 2010; Asokbunyarat et al., 2015). Papandreou et al. (2011) studied the adsorption capacity of fly ash porous pellets to remove Pb, Zn, and Cr, and the adsorption process was irreversible in alkaline solutions. During the batch experiment, the pH of the aqueous solution ranged from 9 to 10 after the pellets were placed in it. Hence, the potential heavy metal adsorption capacity of FAP and BAP could also reduce the heavy metal content in water to a certain extent. Comparing the performance between FAPs and BAPs, the BAPs had higher P adsorption capacity and less heavy metal leaching than that of FAP, which indicated the BAP to be more suitable P adsorbent than FAP.

In general, this study indicated that FAPs and BAPs can be effectively used as the P adsorbents but the potential of heavy metal leaching should be also considered for FAPs. The proposed pelleting process with different mix material proportion to make FAPs and BAPs is expected as a clean and feasible approach to dispose of coal fly ash and bottom ash compared to dump them in the landfill. Meanwhile, there are two aspects needs to be explored in the future: (1) since the post-processing is also vital for the development of pellet adsorbent, it is necessary to reveal the possibility of P-containing pellets as the potential fertilizers to provide alternative phosphorus sources in phosphate recovery. (2) pH is a critical parameter that affects zeta potential of the pellets; further investigation is needed to identify the effect of the point of zero charge of these pellets on pellets' surface adsorption.

5. Conclusion

In this study, a series of fly ash pellets (FAPs) and bottom ash pellets (BAPs) containing varying Sodium Dodecyl Sulfate (SDS, foaming agent) proportion, were prepared and applied to remove phosphate ion (P) from the aqueous solution. The results demonstrated that the foaming treatment enhanced the adsorption capacity of phosphate by

enhancing the porosity and surface structure in pellets. The FAP with 4% SDS and the BAP with 6% SDS resulted in the highest P removal. By increasing pellets porosity using SDS can synergistically improve the physisorption and chemisorption capacities. Freundlich isotherm depicted the best fit to FAP absorption phenomenon, while the Langmuir isotherm was more suitable to the BAP. The increase in pH had a positive influence on phosphate adsorption performance. Leaching tests indicated that pelleting processes could significantly reduce the heavy metals released from the pellets. Therefore, using fly ash and bottom ash as pelletized-adsorbents can be an eco-friendly scheme for coal ashes reuse and water quality remediation but the potential of heavy metal leaching should be considered for FAP before using it.

Acknowledgements

This work was supported by the USDA National Institute of Food and Agriculture, Hatch project ILLU-741-379. We also acknowledge support provided by a grant (741119) from Student Sustainability Committee at the University of Illinois for the materials and sample analysis for this study. We appreciate the scholarship provided by China Scholarship Council to Hongxu Zhou to conduct this study. We are grateful to Dr. Kiran Subedi for his assistance in ICP-MS analysis.

Appendix A. Supplementary data

Supplementary material related to this article can be found, in the online version, at doi:https://doi.org/10.1016/j.resconrec.2019.06.017.

References

Agriz, C., Moragues, A., Menéndez, E., 2018. Use of ground coal bottom as cement constituent in concretes exposed to chloride environments. J. Clean. Prod. 170, 25–33. https://doi.org/10.1016/j.jclepro.2017.09.117.

Ahmaruzzaman, M., 2010. A review on the utilization of fly ash. Prog. Energy Combust. Sci. 36 (3), 327–363. https://doi.org/10.1016/j.pecs.2009.11.003.

Allred, B.J., 2010. Laboratory batch test evaluation of five filter materials for removal of nutrients and pesticides from drainage waters. Trans. ASABE 53 (1), 39–54. https://doi.org/10.13031/2013.29501.

Asl, S.M.H., Javadian, H., Khavarpour, M., Belviso, C., Taghavi, M., Mafhsudi, M., 2019. Porous adsorbents derived from coal fly ash as cost-effective and environmentally-friendly sources of aluminosilicate for sequestration of aqueous and gaseous pollutants: a review. J. Clean. Prod. 208, 1131–1147. https://doi.org/10.1016/j.jclepro.2018.10.186.

Asokbunyarat, V., van Hullebusch, E.D., Lens, P.N.L., Annachhatre, A.P., 2015. Coal bottom ash as sorbing material for Fe (II), Cu (II), Mn (II), and Zn (II) removal from aqueous solutions. Water Air Soil Pollut. 226 (5), 143. https://doi.org/10.1007/s11270-015-2415-5.

Badruzzaman, M., Westerhoff, P., Knappe, D.R.U., 2004. Intraparticle diffusion and adsorption of arsenate onto granular ferric hydroxide (GFH). Water Res. 38 (18), 4002–4012. https://doi.org/10.1016/j.watres.2004.07.007.

Chen, J., Cai, Y., Clark, M., Yu, Y., 2013. Equilibrium and kinetic studies of phosphate from solution onto a hydrothermally modified oyster shell material. PLoS One 8, e60243. https://doi.org/10.1371/journal.pone.0060243.

Chen, M., Wang, N., Yu, J., Yamaguchi, A., 2007. Effect of porosity on carbonation and hydration resistance of Cao materials. J. Eur. Ceram. Soc. 27 (4), 1953–1959. https://doi.org/10.1016/j.jeurceramsoc.2006.05.101.

Chimenos, J.M., Segarra, M., Fernández, M.A., Espiell, F., 1999. Characterization of the bottom ash in municipal solid waste incinerator. J. Hazard. Mater. 64, 211–222. https://doi.org/10.1016/S0304-3894(98)00246-5.

Chong, M.F., Lee, K.P., Chieng, H.J., Syazwani Binti Ramli, I.I., 2009. Removal of boron from ceramic industry wastewater by adsorption-flocculation mechanism using palm oil mill boiler (POMB) bottom ash and polymer. Water Res. 43 (13), 3326–3334. https://doi.org/10.1016/j.watres.2009.04.044.

Colangelo, F., Cioffi, R., Montagnaro, F., Santoro, L., 2012. Soluble salt removal from MSWI fly ash and its stabilization for safer disposal and recovery as road basement material. Waste Manag. 32 (6), 1179–1185. https://doi.org/10.1016/j.wasman.2011.12.013.

Conley, Hans W.Paerl, Howarth, Robert W., Boesch, Donald F., Seitzinger, Sybil P., Havens, Karl E., Lancelot, Christiane, Likens, G.E., 2009. Ecology controlling eutrophication: nitrogen and phosphorus. Science 323, 1014–1015. https://doi.org/10.1126/science.1167755.

Cui, X.Q., Li, H., Yao, Z.Y., Shen, Y., He, Z.L., Yang, X., Ng, H.Y., Wang, C.H., 2018. Removal of nitrate and phosphate by chitosan composited beads derived from crude oil refinery waste: sorption and cost-benefit analysis. J. Clean. Prod. 207, 846–856. https://doi.org/10.1016/j.jclepro.2018.10.027.

Dai, L.C., Tan, F.R., Li, H., Zhu, N.M., He, M.X., Zhu, Q.L., Hu, G.Q., Wang, L., Zhao, J., 2017. Calcium-rich biochar from the pyrolysis of crab shell for phosphorus removal. J. Environ. Manag. 198, 70–74. https://doi.org/10.1016/j.jenvman.2017.04.057.

Gan, F.Q., Zhou, J.M., Wang, H.Y., Du, C.W., Chen, X.Q., 2009. Removal of phosphate from aqueous solution by thermally treated natural palygorskite. Water Res. 43 (11), 2907–2915. https://doi.org/10.1016/j.watres.2009.03.051.

Guo, B., Liu, B., Yang, J., Zhang, S.G., 2017. The mechanisms of heavy metal immobilization by cementitious material treatments and thermal treatments: a review. J. Environ. Manag. 193, 410–422. https://doi.org/10.1016/j.jenvman.2017.02.026.

Gustafsson, J.P., Mwamila, L.B., Kergoat, K.évin., 2012. The pH dependence of phosphate sorption and desorption in Swedish agricultural soils. Geoderma 189-190, 304–311. https://doi.org/10.1016/j.geoderma.2012.05.014.

Han, Y., Kim, H.J., Park, J., 2011. Fabrication and characterization of macro-porous flyash ceramic pellets. Mater. Charact. 62 (9), 817–824. https://doi.org/10.1016/j.matchar.2011.05.014.

Hermassi, M., Valderrama, C., Moreno, N., Font, O., Querol, X., Batis, N.H., Cortina, J.L., 2017. Fly ash as reactive sorbent for phosphate removal from treated waste water as a potential slow release fertilizer. J. Environ. Chem. Eng. 5 (1), 160–169. https://doi.org/10.1016/j.jece.2016.11.027.

Huang, W.Y., Zhang, Y.M., Li, D., 2017. Adsorptive removal of phosphate from water using mesoporous materials: a review. J. Environ. Manag. 193, 470–482. https://doi.org/10.1016/j.jenvman.2017.02.030.

Khelifi, O., Kozuki, Y., Murakami, H., Kurata, K., Nishioka, M., 2002. Nutrients adsorption from seawater by new porous carrier made from zeolitized fly ash and slag. Mar. Pollut. Bull. 45 (1), 311–315. https://doi.org/10.1016/S0025-326X(02)00107-8.

Koukouzas, N., Vasilatos, C., Itskos, G., Mitsis, I., Moutsatsou, A., 2010. Removal of heavy metals from wastewater using CFB-coal fly ash zeolitic materials. J. Hazard. Mater. 173 (1-3), 581–588. https://doi.org/10.1016/j.jhazmat.2009.08.126.

Kundu, S., Gupta, A.K., 2006. Arsenic adsorption onto iron oxide-coated cement (IOCC): regression analysis of equilibrium data with several isotherm models and their optimization. Chem. Eng. J. 122 (1), 93–106. https://doi.org/10.1016/j.cej.2006.06.002.

Lakshmi, V., Resmi, V.G., Raju, A., Deepa, J.P., Rajan, T.P.D., Pavithran, C., Pai, B.C., 2015. Concentration dependent pore morphological tuning of kaolin clay foams using sodium dodecyl sulfate as foaming agent. Ceram. Int. 41 (10), 14263–14269. https://doi.org/10.1016/j.ceramint.2015.07.056.

Lemly, A.D., 2015. Damage cost of the Dan River coal ash spill. Environ. Pollut. 197, 55–61. https://doi.org/10.1016/j.envpol.2014.11.027.

Li, S., Cooke, R.A., Huang, X.F., Christianson, L., Bhattarai, R., 2018. Evaluation of fly ash pellets for phosphorus removal in a laboratory scale denitrifying bioreactor. J. Environ. Manag. 207, 269–275. https://doi.org/10.1016/j.jenvman.2017.11.040.

Li, S., Cooke, R.A., Wang, L., Ma, F., Bhattarai, R., 2017. Characterization of fly ash ceramic pellet for phosphorus removal. J. Environ. Manag. 189, 67–74. https://doi.org/10.1016/j.jenvman.2016.12.042.

Lin, C.Y., Yang, D.H., 2002. Removal of pollutants from wastewater by coal bottom ash. J. Environ. Sci. Health A. Tox. Subst. Environ. Eng. 37 (8), 1509–1522. https://doi.org/10.1081/ESE-120013273.

Littler, J., Geroni, J.N., Sapsford, D.J., Coulton, R., Griffiths, A.J., 2013. Mechanisms of phosphorus removal by cement-bound ochre pellets. Chemosphere 90 (4), 1533–1538. https://doi.org/10.1016/j.chemosphere.2012.08.054.

Lu, S.G., Bai, S.Q., Zhu, L., Shan, H.D., 2009. Removal mechanism of phosphate from aqueous solution by fly ash. J. Hazard. Mater. 161 (1), 95–101. https://doi.org/10.1016/j.jhazmat.2008.02.123.

Lu, X.W., Shih, K., 2012. Metal stabilization mechanism of incorporating lead-bearing sludge in kaolinite-based ceramics. Chemosphere 86 (8), 817–821. https://doi.org/10.1016/j.chemosphere.2011.11.043.

Mor, S., Chhoden, K., Ravindra, K., 2016. Application of agro-waste rice husk ash for the removal of phosphate from the wastewater. J. Clean. Prod. 129, 673–680. https://doi.org/10.1016/j.jclepro.2016.03.088.

National Primary Drinking Water Regulations (NPDWR), 2009. United States Environmental Protection Agency, EPA 816-F-09-004, May 2009.

Papandreou, A.D., Stournaras, C.J., Panias, D., Paspaliaris, I., 2011. Adsorption of Pb (II), Zn (II) and Cr (II) on coal fly ash porous pellets. Min. Eng. 24 (13), 1495–1501.

Pengthamkeerati, P., Satapanajaru, T., Chularuengoaksorn, P., 2008. Chemical modification of coal fly ash for the removal of phosphate from aqueous solution. Fuel 87 (12), 2469–2476. https://doi.org/10.1016/j.mineng.2011.07.016.

Ragheb, S.M., 2013. Phosphate removal from aqueous solution using slag and fly ash. HBRC J. 9 (3), 270–275. https://doi.org/10.1016/j.hbrcj.2013.08.005.

Ren, X.J., Sancaktar, E., 2019. Use of fly ash as eco-friendly filler in synthetic rubber for tie applications. J. Clean. Prod. 206, 374–382. https://doi.org/10.1016/j.jclepro.2018.09.202.

Rangabhashiyam, S., Anu, N., Nandagopal, M.S.G., Selvaraju, N., 2014. Relevance of isotherm models in biosorption of pollutants by agricultural byproducts. J. Environ. Chem. Eng. 2 (1), 398–414. https://doi.org/10.1016/j.jece.2014.01.014.

Sabbas, T., Polettini, A., Pomi, R., Astrup, T., Hjelmar, O., Mostbauer, P., Cappai, G., Magel, G., Salhofer, S., Speiser, C., Heuss-Assbichler, S., Klein, R., Lechner, P., 2003. Management of municipal solid waste incineration residues. Waste Manag. 23 (1), 61–88. https://doi.org/10.1016/S0956-053X(02)00161-7.

Song, H.S., Kim, C.H., 1990. The effect of surface carbonation on the hydration of Cao. Cem Concr Res. 20 (5), 815–823. https://doi.org/10.1016/0008-8846(90)90015-P.

Su, M., Liao, C., Chuang, K.H., Wey, M.Y., Shih, K., 2015. Cadmium stabilization efficiency and leachability by cdal4o7 monoclinic structure. Environ. Sci. Technol. 49 (24), 14452–14459. https://doi.org/10.1021/acs.est.5b02072.

Sun, W.L., Qu, Y.Z., Yu, Q., Ni, J.R., 2008. Adsorption of organic pollutants from coking and papermaking wastewaters by bottom ash. J. Hazard. Mater. 154 (1), 595–601. https://doi.org/10.1016/j.jhazmat.2007.10.063.

Singh, N.M.M., Arya, S., 2019. Utilization of coal bottom ash in recycled concrete aggregates based self compacting concrete blended with metakaolin. Resour. Conserv. Recycl. 144, 240–251. https://doi.org/10.1016/j.resconrec.2019.01.044.

USEPA, 1995. Ecological Restoration: a Tool to Manage Stream Quality. Report EPA 841-F-95-007. US EPA, Washington, DC, USA.

USEPA, 1993. Methods for the Determination of Inorganic Substances in Environmental Samples. 202.1, 215.1, 236.1, 242.1, and 365.1. USEPA, Washington, DC.USA.

Van Gervem, T., Van Keer, E., Arickx, S., Jaspers, M., Wauters, G., Vandecasteele, C., 2005. Carbonation of MSWI-bottom ash to decrease heavy metal leaching, in view of recycling. Waste Manag. 25 (3), 291–300. https://doi.org/10.1016/j.wasman.2004.07.008.

Wang, S.B., Soudi, M., Li, L., Zhu, Z.H., 2006. Coal ash conversion into effective adsorbents for removal of heavy metals and dyes from wastewater. J. Hazard. Mater. 133 (1-3), 243–251. https://doi.org/10.1016/j.jes.2016.04.025.

Wei, X., Viadero, R.C., Bhojappa, S., 2008. Phosphorus removal by acid mine drainage sludge from secondary effluents of municipal wastewater treatment plants. Water Res. 42 (13), 3275–3284. https://doi.org/10.1016/j.watres.2008.04.005.

Xuan, D., Poon, C.S., 2017. Removal of metallic Al and Al/Zn alloys in MSWI bottom ash by alkaline treatment. J. Hazard. Mater. 344, 73–80. https://doi.org/10.1016/j.jhazmat.2017.10.002.

Xu, G., Shi, X., 2018. Characteristics and applications of fly ash as a sustainable construction material: a state-of-the-art review. Resour. Conserv. Recycl. 136, 95–109. https://doi.org/10.1016/j.resconrec.2018.04.010.

Yang, J., Wang, S., Lu, Z.B., Yang, J., Lou, S.J., 2009. Converter slag-coal cinder columns for the removal of phosphorous and other pollutants. J. Hazard. Mater. 168 (1), 331–337. https://doi.org/10.1016/j.jhazmat.2009.02.024.

Zhang, Z.Q., He, F., Zhang, Y.L., Yu, R.J., Gao, Z.Q., 2017. Experiments and modelling of potassium release behavior from tablet biomass ash for better recycling of ash as eco-friendly fertilizer. J. Clean. Prod. 170, 379–387. https://doi.org/10.1016/j.jclepro.2017.09.150.